Research Article

Prediction of the Mechanical Properties of Fibre-Reinforced Quarry Dust Concrete Using Response Surface and Artificial Neural Network Techniques

Jayaprakash Sridhar [ID],[1] **Shanmugam Balaji** [ID],[2] **Dhanapal Jegatheeswaran,**[3] **and Paul Awoyera** [ID][4]

[1]*Department of Civil Engineering, GMR Institute of Technology, Rajam, Andhra Pradesh, India*
[2]*Department of Civil Engineering, Kongu Engineering College, Perundurai, Tamil Nadu, India*
[3]*Department of Civil Engineering, Sona College of Technology, Salem, Tamil Nadu, India*
[4]*Department of Civil Engineering, Covenant University, Ota, Nigeria*

Correspondence should be addressed to Jayaprakash Sridhar; sridharjayaprakash@gmail.com

The focus of this study is to forecast the 28-day compressive strength and split tensile strength of concrete with various percentages of jute and coconut fibres mixed with quarry dust. The response surface methodology (RSM) and the artificial neural networks (ANN) methods were adopted for 3 variable process modelling (coconut fibres of 0% to 2.5%, jute fibres of 0% to 2.5%, and quarry dust of 0% to 25% by weight of cement). The RSM Box−Behnken design (BBD) method was adopted to design the experiments. Test results showed that compressive strength of 34.6 N/mm^2 was obtained for concrete with 0% jute, 0% coir, and 12.5% quarry dust. Similarly, the maximum split tensile strength of 3.8 N/mm^2 was obtained for concrete with 1.25% jute fibres, 1.25% coconut fibres, and 12.5% quarry dust. ANOVA and Pareto charts were used to assess regression models for response data. Each progression variable's statistical significance was assessed, and the resulting models were expressed as second-order polynomial equations. Levenberg−Marquardt (LM) algorithm with feed-forward back propagation neural network was used for assessing the compressive strength and split tensile strength of concrete. The statistical data, root mean square error (RMSE), mean absolute error (MAE), mean absolute and percentage error (MAPE), and determination coefficient (R^2) show that both techniques, ANN and RSM, are effective tools for predicting compressive strength and split tensile strength. Furthermore, RSM and ANN models have a high correlation with experimental data. However, the response surface methodology model is more accurate.

1. Introduction

Over many decades, concrete has been the most often used building material in the world, and its use in the construction sector has steadily increased. This situation is possible due to its strength, toughness, and affordability. However, its use has been constrained because of its susceptibility to fragility under stiffness, a meager resistance to cracking, and low fracture strain capacity. To overcome this fragile behaviour of plain concrete and issues relating to the shortage of raw materials, fibre-reinforced concrete with quarry dust has considered an alternative. Concrete with a higher percentage of recycled aggregate decreases the compressive strength from 22.62% to 18.56%. The predicted results using ANN reveal that it is an effective tool [1]. Three variable process modelling may be utilised to forecast compressive strength utilising response surface methodology (RSM) and artificial neural networks (ANN) [2]. Related to other models, the RSM model's prediction of compressive strength using nondestructive testing has high accuracy [3]. The use of RSM is simpler than any basic formula and offers an effective output for predicting the strength of concrete

proportioning. Moreover, concrete strength properties can be estimated from established ANN [4]. RSM needs no calibration, which is a promising tool for strength prediction, while ANN needs calibration to get the best accuracy [5]. Mechanical properties of concrete decrease with a complex percentage substitution of quarry dust, while abrasion resistance and sorptivity properties increase with a 30% replacement of quarry dust and metakaolin [6, 7]. The fresh concrete properties increase with addition of 0.50% of jute fibres, and on the other hand, hardened properties increase with 0.25% of jute fibres [8]. Concrete with 25% of quarry dust has a 7.9% higher modulus of elasticity, while 100% of sand substitution with quarry dust has 8.6% less modulus of elasticity [9]. Compressive strength and split tensile strength of 26.4 Mpa and 26.1 Mpa, respectively, were achieved for concrete containing 1.5% bamboo and 2% jute fibres by weight of cement. SEM analysis exposes that the breaking of fibres is due to debonding of fibres from the concrete matrix [10]. Concrete with combined micro and macro fibres enhances the mechanical properties of concrete [11]. When glass powder is substituted for cement by 5% and plastic waste by 10%, the mechanical properties of the concrete rise [12]. The compressive strength of concrete increases by 50% for 20% replacement of quarry dust for sand and flexural strength, and split tensile strength decreases by 25% for 20% replacement when compared with conventional concrete [13]. The addition of chopped jute fibres in M25 concrete of 1.5% by weight of cement increases the compressive strength by 19.7%, and tensile strength increases by 30.8% at 28 days of curing. The workability of concrete reduces by 1.5% due to the hydrophilic nature of jute fibre [14]. The compressive strength of concrete is increased by 84.27% when paraffin-coated coconut fibre makes up 0.5% of the cement weight [15]. The addition of jute fibres has effectively filled the microcracks in the concrete thereby reducing the porosity of the concrete and preventing the propagation of cracks [16]. Steel and polymer fibres increase the flexural capacity of RC beams, whereas the glass fibres addition has less influence on concrete as it increases the strength only by 5% [17]. Ultimate load and ductility of concrete containing macro synthetic fibres [18] increase. Artificial fibres pose health and environmental risks in addition to being expensive. Natural fibres are small-diameter discrete and are dispersed randomly in concrete. They benefit the environment, economy, and conservation in terms of energy and resources [8, 19]. The combined effects of silica fume and steel fibres in concrete have significantly improved the mechanical characteristics though concurrently lowering the elastic modulus. Test findings show that silica fume and sisal fibres may be used to strengthen concrete, and they also show an improvement in the material's mechanical qualities for M30 and M40 concrete [20, 21]. The typical range of optimum dose of Jute fibres varies from 1% to 2% depending on the length and diameter of jute fibres [22]. Coconut fibre enhanced the mechanical performance of concrete by preventing cracks, similar to synthetic fibres, but decreased the flowability of concrete [23]. RSM offers statistically proven prediction models that may be adjusted to obtain the best process

configurations. RSM is often beneficial when many factors impact one or more performance attributes or reactions. It may also be used to optimise one or more responses to fulfill a set of requirements. More crucially, RSM allows for adequate experimental interpretation of the nonlinear response surfaces of experimental data [24, 25]. RSM has various benefits for optimization over the one component-at-a-time strategy, which is time-consuming and does not account for factor interaction [26]. Design of experiments (DOE), ideally known as response surface methodology, is used to explore the impact of self-governing factors on outcomes with minimum experiments. It is generally utilised in concrete technology because to its precision in generating precise results [2, 27–29]. Because of the construction of a model with strong performance, ANN is increasingly being used to handle a wide range of civil engineering and material science challenges. To circumvent the drawbacks of the empirical approach, an artificial neural network (ANN) has been employed in many engineering applications in modelling of nonlinear multivariate interrelationships of the behaviour of concrete strength and setting time. The ability of artificial neural networks to learn from the display of sample data sets (patterns), which expresses the system behaviour, is one of their most important qualities [30]. In this study, two models namely Box Behnken Design (BBD) of RSM and Levenberg–Marquardt (NN-LM) algorithm with feed-forward back propagation neural network was developed and compared to predict the compressive strength, split tensile strength of fibre reinforced concrete having of quarry dust, jute, and coconut fibres. The coefficient of determination (R^2), root mean square error (RMSE), mean square error (MSE), mean absolute error (MSE), and mean absolute and percentage error (MAPE) of both models were compared to assess the efficiency of each method. To our knowledge, this is the first report comparing RSM and ANN in the prediction of the compressive strength and split tensile strength of concrete containing jute and coconut fibres.

2. Materials

In this examination, OPC of grade 53, specified by IS 12269-2013 [31], was employed. Its initial setting time was 30 minutes, and its specific gravity was 3.2. Fine aggregate with specific gravity 2.69 conforming to zone III as per IS 10262 2019 [32] and 20 mm coarse aggregate with specific gravity 2.81 were used in the mixture. The quarry dust used for fractional replacement for sand was collected from a local area crusher with a specific gravity of 2.5. Naturally available untreated jute and coconut fibres having 0.2 mm diameter, as shown in Figure 1, are used to prepare the concrete.

2.1. Mix Proportion. The mix proportion utilised in making concrete specimens is 1 : 1.61 : 3.04 at a continual W/C of 0.48. The replacement of sand by quarry dust was done from 0% to 25%. At the same time, the substitution of jute and coconut fibres content was made from 0% to 2.5%.

(a)

(b)

Figure 1: (a) Coconut fibres; (b) jute fibres.

2.2. Test Methods.

The concrete mix was cast in a cubical mould of size $150 \times 150 \times 150$ mm for compressive test, and for splitting tensile strength, a cylindrical mould of diameter 150 mm and height 300 mm was used. Concrete was placed into the mould in 3 layers, and each layer was compacted manually with 25 blows of a tamping rod. The concrete samples were detached from moulds after drying for 24 hrs and kept at room temperature. A total of 45 concrete cube specimens and 45 cylinders were cast for testing experimentally, with 3 samples tested per mix at each curing age. The average of triplicate strength values was taken as the concrete strength. After twenty-eight days, the concrete specimens were removed and tested using a compression testing machine for compressive and split tensile tests.

3. Mathematical Models

3.1. Response Surface Methodology.

Response surface methodology (RSM) discovers the association between several illustrative variables and one or more output variables by analysing the design of experiments. The DoE aims to select the most suitable points where the response should be well examined. Response surface optimization aids in adjusting the experimental circumstances that yield the best response [33]. Response surface methodology (RSM) efficiently optimises trials by taking into account both statistical and mathematical approaches for analysis to compute the total number of experimental data for better performance [34, 35]. In circumstances where there are multiple variables, RSM can be used to investigate the impact of each variable and their interactions on answers (properties), as well as the relevance of each variable in the replies or models [36]. Under experimental designs of BBD, Box–Behnken of 3-factor design was adopted. BBD was adopted to study the effects of mix factors, including quarry dust, coconut fibres, and jute fibre on the mechanical characteristics of concrete. The independent variables were jute fibre (X_1), coconut fibre (X_2), and quarry dust (X_3), and the designed responses were the compressive strength fcs_{28} and split tensile strength $fSTS_{28}$. The obtained response is expressed as shown in equation (1).

$$y = f(X_1, X_2, X_3). \tag{1}$$

A second-order model was developed, as arrayed in equation (2), to elucidate the numerous mechanical properties of concrete and to comprehend the link between the response function and the combined factors as shown as follows:

$$y = k_0 + \sum k_i \quad x_i + \sum k_i \quad x_i 2 + \sum \sum k_{ij} x_i x_j, \tag{2}$$

where y = required response variable; k_0, ki, kj, kij = regression coefficients. The coefficient of determination R^2 helps determine the accuracy of the arrived equation. Factors and levels of variables required are given in Table 1, which is for the two responses in DOE of RSM autonomous variables. The three-factor BBD approach was applied to 15 mixes to ascertain the effects of jute fibres, coconut fibres, and quarry dust on the strength qualities of concrete, as shown in Table 2.

A regression equation (having factors such as linear, interactive, and quadratic coefficients) was used to find the optimum response. To perform this investigation, 15 trials were obtained from RSM and their mix composition is shown in Table 2.

3.2. Artificial Neural Network.

ANN is a computational framework comprising input layers, hidden layers, and output layers. This prediction method is proven to be quite useful for the correct forecasting of output variables in modelling. The primary advantage of the ANN tool is its ability to provide precise modelling for nonlinear models with numerous inputs. Furthermore, ANN tools are widely used because of their ability to deal with inconsistent and unreliable data, as well as their fault tolerance and sturdiness [37, 38]. They comprise a large number of basic handling units which are wired together in a complex communication network. These layers have many dense interconnected units called neurons. The communication between neurons is made with interconnected relations between neurons. To obtain a single output through equation (3), the neurons are multiplied with corresponding weights, added together, and applied to an activation function.

TABLE 1: Levels of variables.

Variables (%)	Minimum (%)	Maximum (%)
Jute fibre	0	2.5
Coconut fibre	0	2.5
Quarry dust	0	25

$$Z = f\left(\sum_{i=0-n} wixi\right) + d \tag{3}$$

where "Z" is the yield from the neuron, "x_i" is the contribution value, "w_i" is the linking weights, "d" is the bias value, and "f" is the initiation function.

In this study, feed-forward propagation of passing the information from contribution nodes is adopted among feed forward and backward propagations. The neural network used for this study is shown in Figure 2.

3.3. Comparison Parameters. Using various statistical studies like the coefficient of correlation (R), coefficient of determination (R^2), root mean square error (RMSE), mean absolute error (MAE), and mean absolute percentage error, the implications of RSM and ANN models were evaluated (MAPE) [39]. The error calculations can be performed using equations (4)–(6).

$$RMSE = \sqrt{\frac{\sum_{1}^{n}(y-x)^2}{n}}, \tag{4}$$

$$MAE = \frac{1}{n}\sum_{1}^{n}|y-x|, \tag{5}$$

$$MAPE = \sum_{1}^{n}|y-x|^*100. \tag{6}$$

Here, x is the real data, y is forecast data, and n is the number of samples.

4. Results and Discussion

4.1. Compressive Strength and Split Tensile Strength. The influence of jute fibres, coconut fibres, and quarry dust under compression at 28 days was studied which are arrayed in Figures 3 and 4. The highest strength under compression of 31.9 N/mm^2 was obtained for JCQD11, having 1.25% jute fibres, 1.25% coconut fibres, and 12.5% quarry dust. Similarly, it is obvious that JCQD07 having 0% jute fibres, 0% coconut fibres, and 12.5% quarry dust has compressive strength of 34.9 N/mm^2. It is evident that adding jute and coconut fibres has a marginal increment in compressive strength. Higher percentage addition of jute and coconut fibres decreases the compressive strength [40]. Due to the JFRCC's high porosity and low specific gravity in comparison to reference concrete, a declining trend in compressive strength was seen when jute fibres were added. Similarly, an extreme split tensile strength of 3.8 N/mm^2 was obtained for JCQD11. The findings demonstrate that the jute and coconut fibres help to increase split tensile strength. Additionally, split tensile strength decreased for concrete specimens containing more than 0.5% by weight of jute and coconut fibres due to the uneven distribution of fibre in the concrete [40].

4.2. RSM Model. Conferring to the BBD, the study was performed to study the influence of the variables jute, coconut fibres, quarry dust to forecast the compressive strength ($f cs_{28}$) and split tensile strength ($f STS_{28}$) of concrete mixes at 28 days. As arrayed in Table 3, experiments were conducted for compressive strength and split tensile strength and the responses that were found were articulated in the equations (7) and (8), and the results are arrayed in Table 3.

$$f cs_{28} = 33.82 - 4.24X_1 - 4.66X_2 + 0.110X_3 + 0.651X_1^2 + 0.175X_2^2 - 0.00491X_3^2 - 0.238X_1 * X_2 - 0.1973X_1 * X_3 + 0.0846X_2 * X_3, \tag{7}$$

$$f STS_{28} = 1.388 + 1.940X_1 + 1.630X_2 + 0.0850X_3 - 0.680X_1^2 - 0.568X_2^2 - 0.00472X_3^2 - 0.352X_1 * X_2 - 0.000X_1 * X_3 + 0.0080X_2 * X_3, \tag{8}$$

where X_1, X_2, X_3 are jute, coconut fibre, and quarry dust, respectively.

4.2.1. Lack of Fit (p Value) and Pareto Analysis. The importance of progression factors is aided by the p value. The likelihood value of the F test, which should be at a minimum, is the p value of the model. If the progression variable's p values are <0.005 and <0.00, respectively, it can be calculated as being considerable. The progression variable is deemed to be insignificant if the p value is greater than 0.005. According to ANOVA Table 4, X_1 has a lower p value than X_2 and X_3,

indicating that jute fibres are an important factor in determining the strength of concrete under compression. The Pareto chart in Figure 5 demonstrates that jute fibre is more significant than coconut fibre and quarry dust for compressive strength at 28 days of curing because its value was greater when compared to the linear (A) and (B&C). Similarly, considering the tensile strength at 28 days from ANOVA Table 4, the quadratic interaction of X_1 and X_2 contributes to tensile strength, of which jute fibres were more substantial and the p value is less than 0.005. Similar observations can be seen from the Pareto chart shown in

TABLE 2: Combinations obtained from RSM model.

| Mix designation	Jute fibres (%) (X_1)	Coconut fibres (%) (X_2)	Quarry dust (%) (X_3)	Fibre length (mm)	Coarse aggregate (kg/m^3)	Fine aggregate (kg/m^3)	Cement (kg/m^3)
JCQD01	0	1.25	0	50	1214.268	642.576	359.210
JCQD02	1.25	1.25	12.5	50	1214.268	642.576	399.125
JCQD03	1.25	2.5	0	50	1214.268	642.576	399.125
JCQD04	1.25	1.25	12.5	50	1214.268	642.576	399.125
JCQD05	2.5	2.5	12.5	50	1214.268	642.576	379.170
JCQD06	2.5	1.25	25	50	1214.268	642.576	379.170
JCQD07	0	0	12.5	50	1214.268	642.576	379.170
JCQD08	0	2.5	12.5	50	1214.268	642.576	399.125
JCQD09	1.25	0	0	50	1214.268	642.576	359.210
JCQD10	1.25	1.25	12.5	50	1214.268	642.576	379.170
JCQD11	0	1.25	25	50	1214.268	642.576	379.170
JCQD12	1.25	0	25	50	1214.268	642.576	359.210
JCQD13	1.25	2.5	25	50	1214.268	642.576	379.170
JCQD14	2.5	1.25	0	50	1214.268	642.576	379.170
JCQD15	2.5	0	12.5	50	1214.268	642.576	359.210
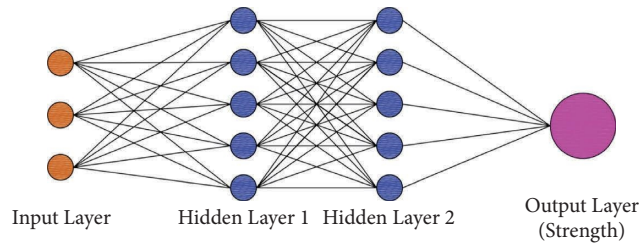
FIGURE 2: Neural network diagram.
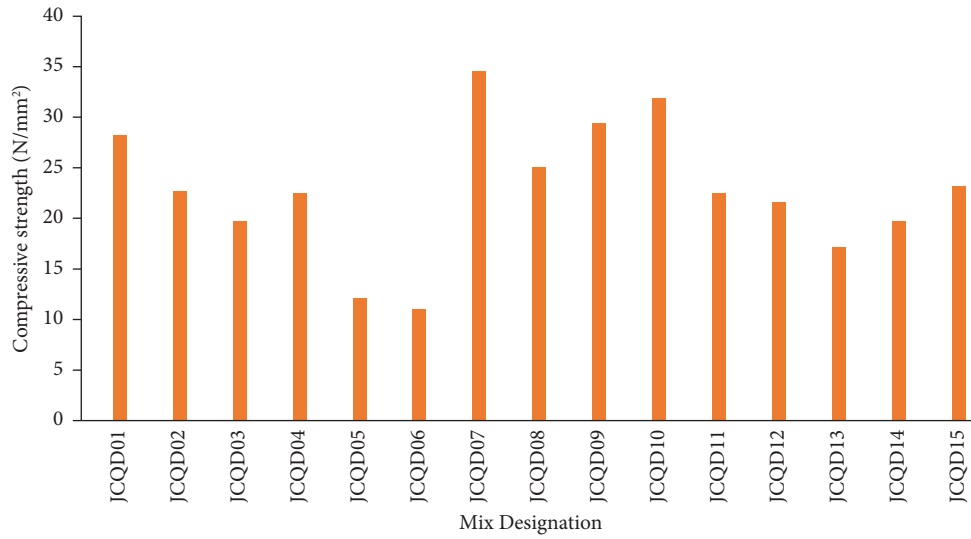
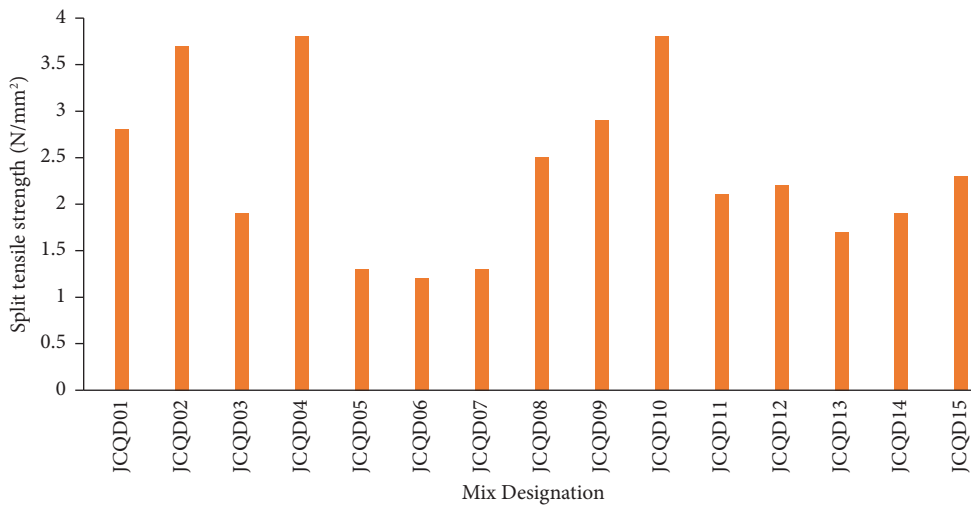FIGURE 3: Concrete compressive strength with jute fibres, coconut fibres, and quarry dust.

FIGURE 4: Concrete split tensile strength with jute fibres, coconut fibres, and quarry dust.

Figure 6. The effect of jute fibre was higher than coconut fibre which is higher than the standard value of 2.57. Because of the bridging action between the concrete and the fibres, the tensile strength of the concrete was increased. From the responses observed, it is concluded that the addition of jute fibres improves both compressive and tensile strength compared to coconut fibres.

4.2.2. Surface Plot Analysis and Optimization of Progression Variables. Figures 7 and 8 show the 3D surface plots to show the impact of jute fibres, coconut fibres, and quarry dust on the responses of compressive strength and split tensile strength. From the figure, it is learned that extreme compressive strength was obtained for 0.5% of jute and coconut fibres from 0.5% with 12.5% of quarry dust at 28 days of

TABLE 3: Predicted strengths.

Mix designation	Jute fibres (%) (X_1)	Coconut fibres (%) (X_2)	Quarry dust (%) (X_3)	$f cs_{28}$ (N/mm^2)	$f STS_{28}$ (N/mm^2)
JCQD01	0	1.25	0	28.25	2.8
JCQD02	1.25	1.25	12.5	22.7	3.7
JCQD03	1.25	2.5	0	19.7	1.9
JCQD04	1.25	1.25	12.5	22.5	3.8
JCQD05	2.5	2.5	12.5	12.17	1.3
JCQD06	2.5	1.25	25	11.02	1.2
JCQD07	0	0	12.5	34.6	1.3
JCQD08	0	2.5	12.5	25.06	2.5
JCQD09	1.25	0	0	29.39	2.9
JCQD10	1.25	1.25	12.5	31.9	3.8
JCQD11	0	1.25	25	22.5	2.1
JCQD12	1.25	0	25	21.6	2.2
JCQD13	1.25	2.5	25	17.2	1.7
JCQD14	2.5	1.25	0	19.7	1.9
JCQD15	2.5	0	12.5	23.2	2.3

TABLE 4: Analysis of variance of RSM model.

Source	Compressive strength ($f cs_{28}$)			Split tensile strength ($f STS_{28}$)		
	DF	F value	p value	DF	F value	p value
Model	9	27.12	0.001	9	8.23	0.016
Linear	3	74.19	0.000	3	3.21	0.121
X_1	1	148.62	0.000	1	3.51	0.120
X_2	1	61.87	0.001	1	1.48	0.278
X_3	1	12.09	0.018	1	4.64	0.084
Square	3	0.92	0.494	3	18.52	0.004
X_1^2	1	1.58	0.265	1	29.25	0.003
X_2^2	1	0.11	0.750	1	20.41	0.006
X_3^2	1	0.90	0.388	1	14.09	0.013
Two way interaction	3	2.98	0.038	3	2.98	0.135
$X_1 * X_2$	1	8.49	0.653	1	8.49	0.033
$X_1 * X_3$	1	0.00	0.011	1	0.00	1.000
$X_2 * X_3$	1	0.44	0.150	1	0.44	0.537

Pareto Chart of the Standardized Effects
(response is COMPRESSIVE STRENGTH, $\alpha = 0.05$)

Factor	Name
A	JUTE FIBRE
B	COCONUT FIBRE
C	QUARRY DUST
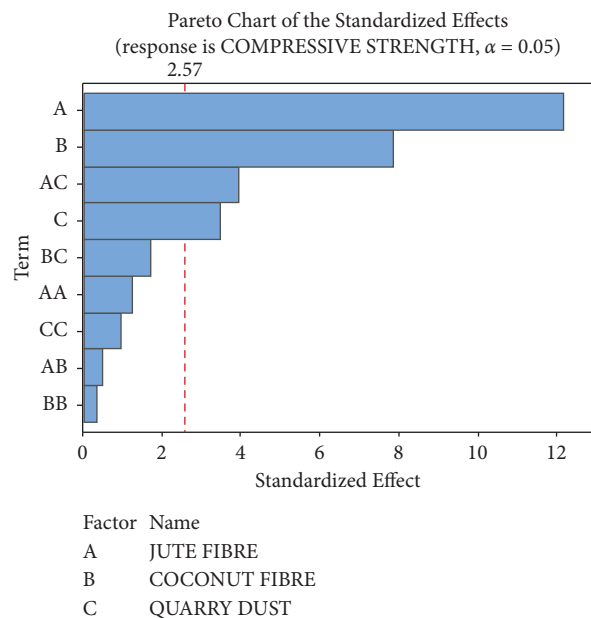
FIGURE 5: Pareto chart for compressive strength.

Pareto Chart of the Standardized Effects
(response is SPLIT TENSILE STRENGTH, $\alpha = 0.05$)

Factor	Name
A	JUTE FIBRE
B	COCONUT FIBRE
C	QUARRY DUST
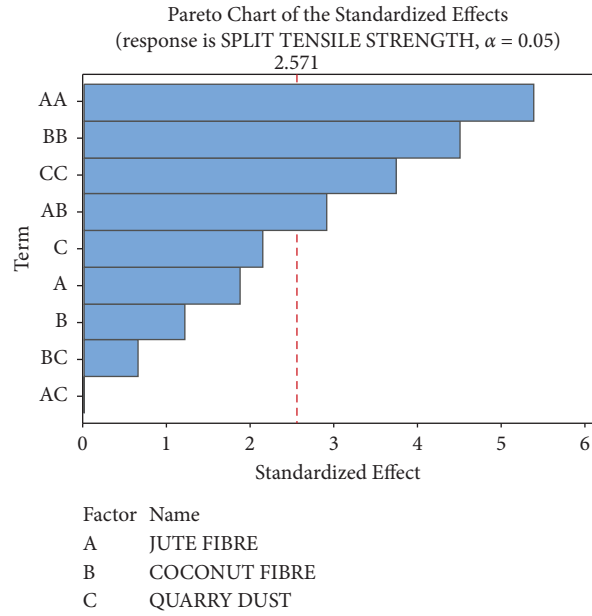
Figure 6: Pareto chart for split tensile strength.

Surface Plots of COMPRESSIVE STRENGTH

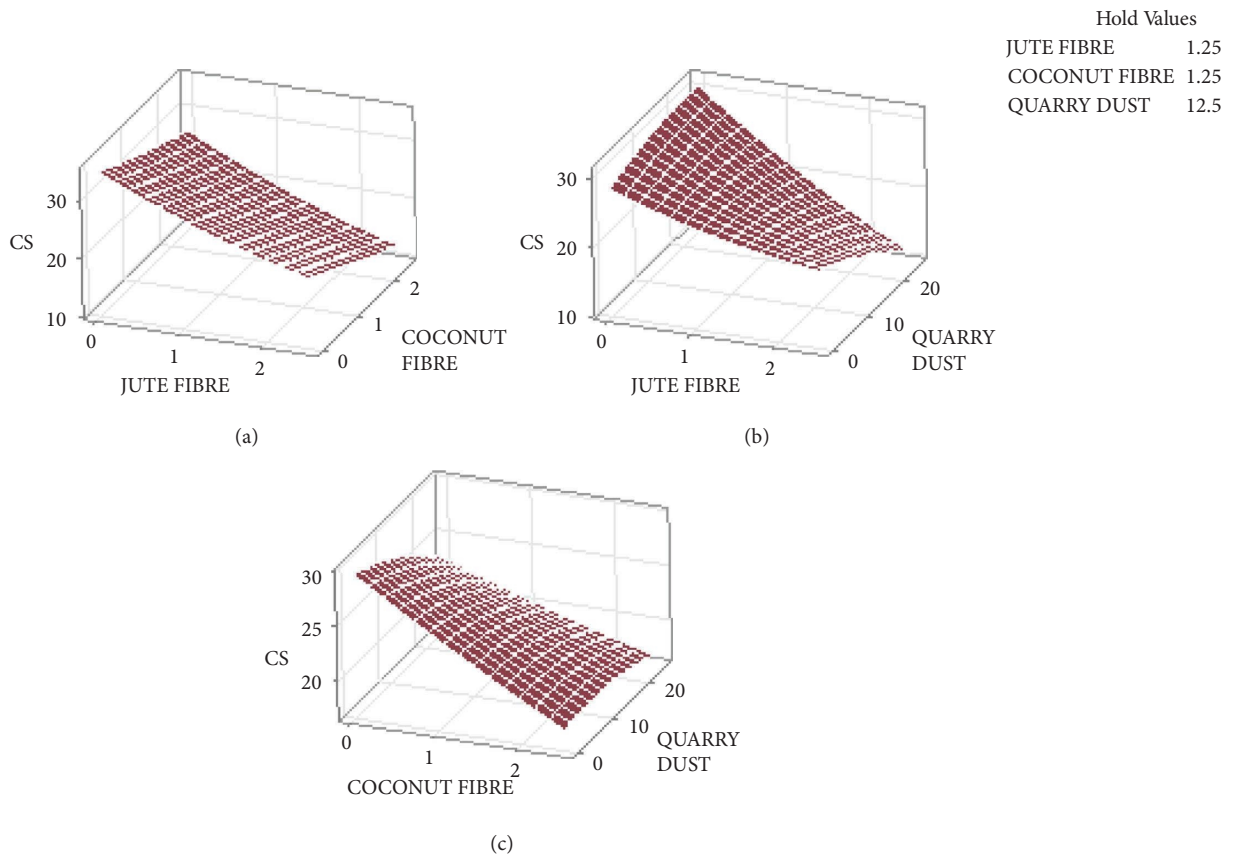| Hold Values	
JUTE FIBRE	1.25
COCONUT FIBRE	1.25
QUARRY DUST	12.5

(a)

(b)

(c)

Figure 7: Surface plots for compressive strength as a function of (a) jute fibre and coconut fibre; (b) jute fibre and quarry dust; (c) coconut fibre and quarry dust.

Surface Plots of SPLIT TENSILE STRENGTH
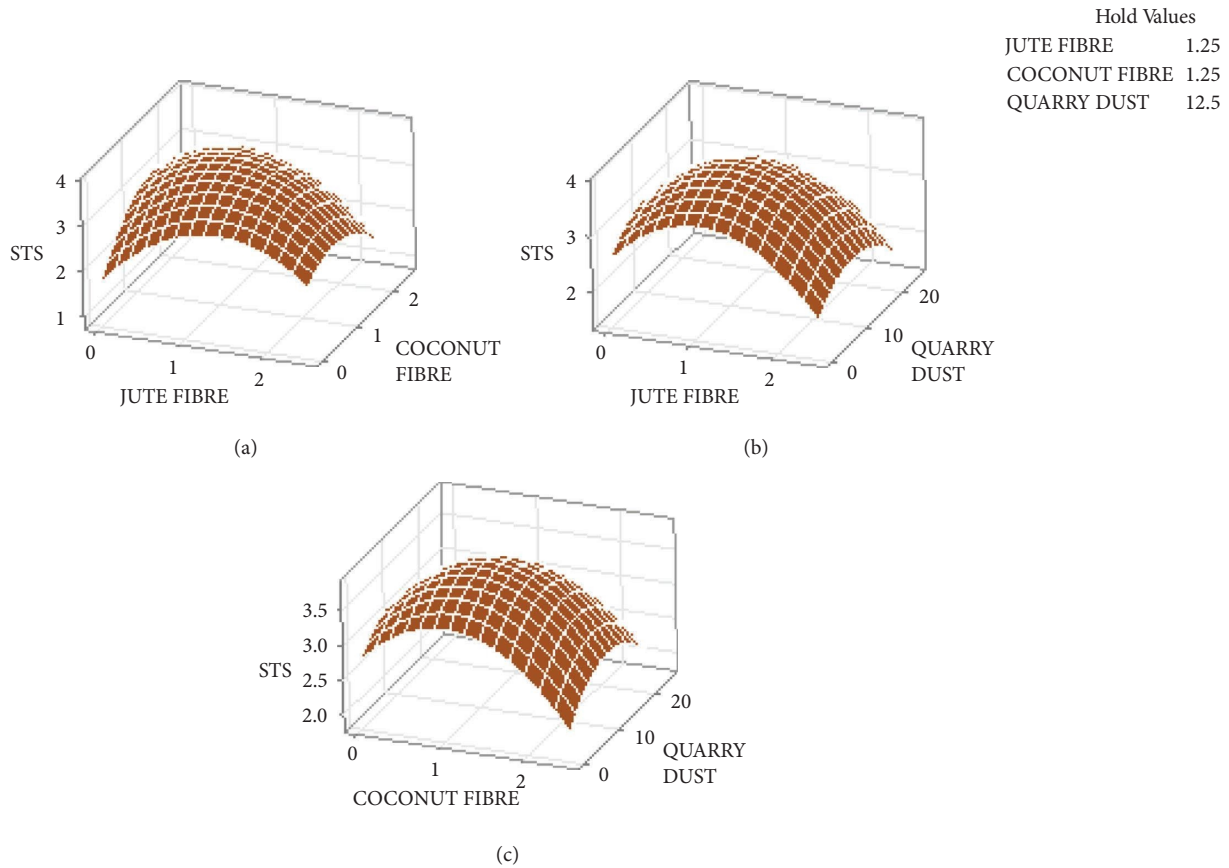
(a)

(b)

(c)

FIGURE 8: Surface plots for split tensile strength as a function of (a) jute fibre and coconut fibre; (b) jute fibre and quarry dust; (c) coconut fibre and quarry dust.

curing, and above 1.25% jute and coconut fibres, the strength decreased. Although adding jute fibres and coconut fibres somewhat improved the compressive strength of concrete, jute fibres had a far more significant impact than quarry dust and coconut fibres after 28 days of curing. Additionally, the compressive strength has decreased when the weight fraction of jute and coconut fibres exceeds 1.25% due to the larger volume of fibre content. The results showed that a suitable accumulation of jute fibre could efficiently fill the microcracks in concrete, reduce the permeability of the concrete structure, and increase the tensile strength and delay the spread of cracks. The optimized strength under compression and split tensile strength is shown in Figure 9. From Figure 9, it can be seen that to attain the highest compressive strength and split tensile strength at 28 days, the optimal value of jute fibres, coconut fibres, and quarry dust were 0.6547%, 0.8081%, and 9.0909%, respectively.

4.3. ANN Model. Compressive strength and split tensile strength were forecast using ANN feed-forward back propagation neural network at 28 days of curing. The model contains 75% of samples deployed for training, and the rest 25% is used for validation and testing set. Jute fibre, coconut fibres, and quarry dust are taken as contribution parameters, compressive strength and split tensile strength are

considered as output layers, and two hidden layers with 10 neurons were selected to make sound ANN models. The outcomes of training and cross-validation are presented in Figure 10, and it reveals a very robust association with $R^2 = 0.88336$ for the training and $R^2 = 0.9994$ for the authentication, where R is the linear correlation coefficient. This shows that the trained neural network is good and accurate.

The competence of the ANN models was determined using the coefficient of determination value by comparing actual data with predicted data.

The anticipated and actual values for compressive strength and split tensile strength, respectively, were equal, demonstrating well-fitted data. A positive correlation between the actual and expected values is shown by the compressive strength and split tensile strength R values, which are both more than 0.9. Additionally, the ANN models that are trained using real data have successfully predicted the outcomes. The predicted strength using RSM and ANN are arrayed in Table 5.

4.4. Validation and Comparison of ANN and RSM Models. The performance of developed RSM and ANN models was estimated by R^2, RMSE, MAE, and MAPE, as shown in Table 6.
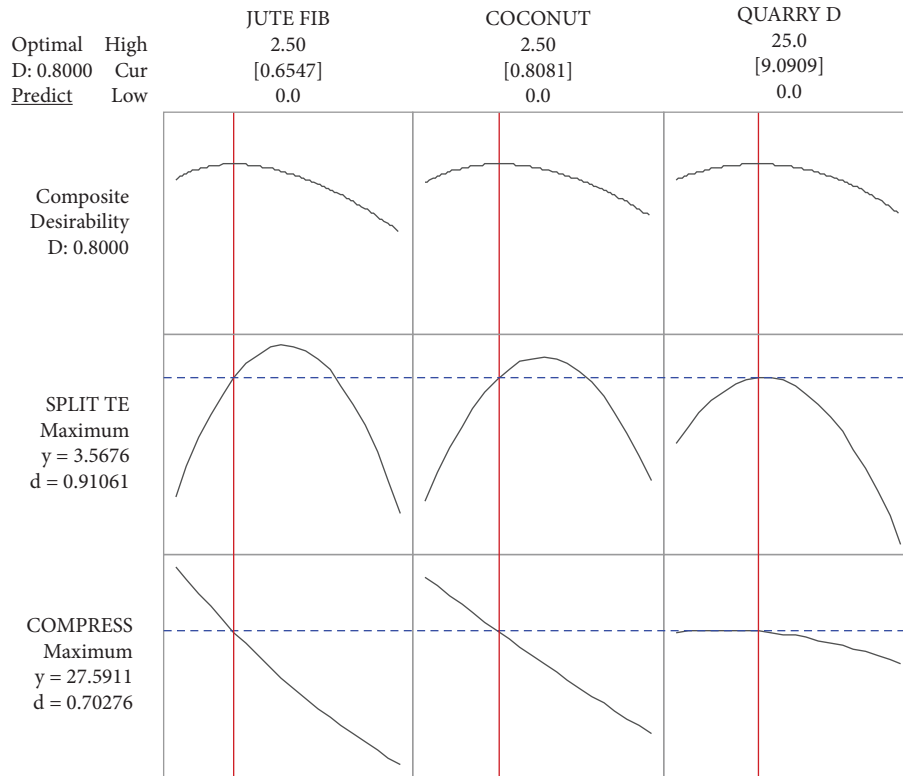
FIGURE 9: Response optimization for compressive and split tensile strengths.
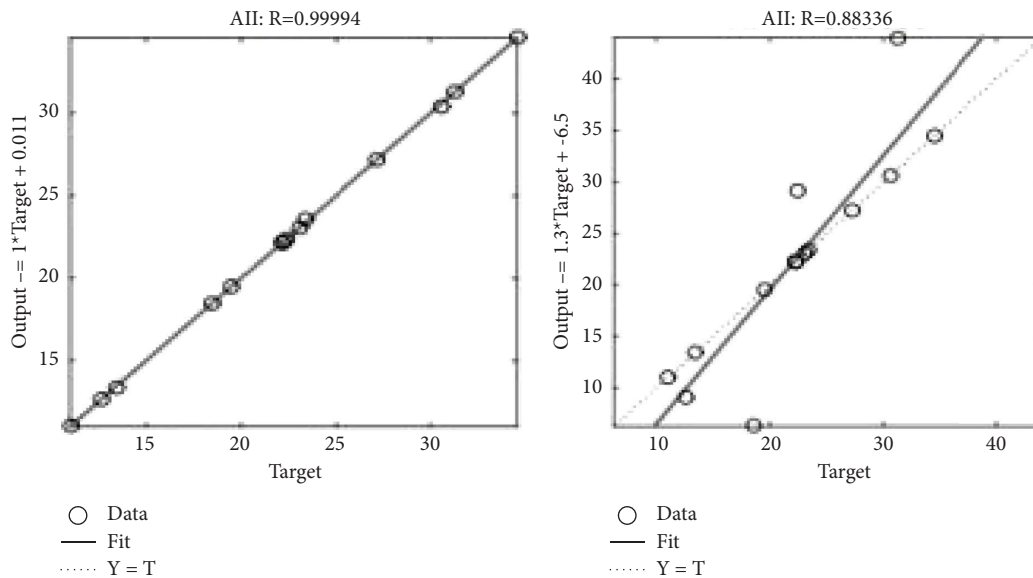

FIGURE 10: Coefficient of determination for training and cross-validation of ANN.

When compared to ANN, RSM showed good accuracy for estimated R^2 for compressive strength and split tensile strength. In all cases, R^2 values are almost 0.9. This suggests that models established by RSM were more operative and forecast the outcomes more exactly. According to the statistical analysis, RSM and ANN models have high-quality

simulations due to their capacity for prediction and their ability to match data effectively. The RSM yet shows strong excellence when compared to ANN, as R^2, RMSE, MAE, and MAPE in overall had shown lower values.

The obtained R^2 values of compressive strength and split tensile strength in RSM are 0.9723 and 0.9368, respectively.

TABLE 5: Predicted strength values of concrete using RSM &ANN.

Sample no	Jute fibres (%) (X_1)	Coconut fibres (%) (X_2)	Quarry dust (%) (X_3)	Compressive strength (N/mm^2)			Split tensile strength (N/mm^2)		
				Exp	RSM	ANN	Exp	RSM	ANN
JCQD01	0	1.25	0	28.25	28.27	28.43	2.8	2.54	2.62
JCQD02	1.25	1.25	12.5	22.7	19.82	20.23	3.7	3.80	2.04
JCQD03	1.25	2.5	0	19.7	18.24	19.12	1.9	2.18	1.98
JCQD04	1.25	1.25	12.5	22.5	19.82	20.22	3.8	3.80	2.03
JCQD05	2.5	2.5	12.5	12.17	7.04	8.13	1.3	0.89	0.88
JCQD06	2.5	1.25	25	11.02	5.70	6.78	1.2	1.46	0.72
JCQD07	0	0	12.5	34.6	34.43	33.44	1.3	1.72	3.42
JCQD08	0	2.5	12.5	25.06	21.23	20.23	2.5	2.49	2.08
JCQD09	1.25	0	0	29.39	29.54	29.45	2.9	2.76	2.88
JCQD10	1.25	1.25	12.5	22.5	19.82	18.98	3.8	3.80	1.88
JCQD11	0	1.25	25	31.9	25.31	26.71	2.1	1.97	2.70
JCQD12	1.25	0	25	21.6	23.05	24.12	2.2	1.93	2.34
JCQD13	1.25	2.5	25	17.2	6.47	8.12	1.7	1.86	0.80
JCQD14	2.5	1.25	0	19.7	20.99	19.19	1.9	2.04	1.91
JCQD15	2.5	0	12.5	23.2	21.73	20.78	2.3	2.31	2.07

TABLE 6: Validation and comparison of RSM and ANN models.

Parameters	RSM (CMP)	RSM (STS)	ANN (CMP)	ANN (STS)
R^2	0.9723	0.9368	0.99994	0.88336
RMSE	0.19735	0.2768	0.12505	0.49061
MAE	0.162845	0.24125	0.106	0.38
MAPE	2.2%	8.5%	1.6%	9.4%

Whereas the R^2 values obtained for compressive strength and split tensile strength in ANN are 0.99994 and 0.88336, respectively. The RMSE values obtained for compressive strength and split tensile strength in RSM and ANN are 0.19735, 0.2768, 0.12505, and 0.49061, respectively. The MAE values obtained for compressive strength and split tensile strength in RSM are ANN are 0.162845, 0.24125, 0.106, and 0.38, respectively. The MAPE values obtained for compressive strength and split tensile strength are 2.2%, 8.5%, 1.6%, and 9.4%, respectively.

5. Conclusion

RSM and ANN were used in this work to analyse the impact of adding natural fibres and quarry dust on the compressive strength and splitting tensile strengths of concrete. The following conclusions were drawn from the study:

(i) Fibre content up to 1.25% by weight of cement increases the split tensile strength due to its binding nature with the concrete. A higher percentage of fibre content decreases the compressive strength as it requires more cement content for proper mixing, leading to a decrease in strength.

(ii) Quarry dust can be used by itself to enhance compressive strength by up to 25%; however, it is not suited to enhance split tensile strength. The

natural fibre addition greatly increases the split tensile strength by reducing the cracks at failure.

(iii) The RSM and ANN models' outputs, which were developed using real data, demonstrate that the models are capable of providing accurate predictions of concrete properties. Results from comparing the two approaches revealed that RSM models outperform ANN in terms of prediction, with a determination coefficient of almost 1.

(iv) The R^2 values obtained for compressive strength and split tensile strength in RSM are 0.9723 and 0.9368, respectively. At the same time, the R^2 values obtained for compressive strength and split tensile strength in ANN are 0.99994 and 0.88336, respectively. The comparison findings demonstrate that the RSM model outperforms the ANN model, with an excellent correlation coefficient (R^2) close to 1.

Data Availability

The datasets used in this research are available upon request from the corresponding author.

Conflicts of Interest

The authors declare that they have no conflicts of interest.

References

[1] S. Ray, M. Haque, T. Ahmed, and T. T. Nahin, "Comparison of artificial neural network (ANN) and response surface methodology (RSM) in predicting the compressive and splitting tensile strength of concrete prepared with glass waste and tin (Sn) can fiber," *Journal of King Saud University - Engineering Sciences*, vol. 209, pp. 425–436, 2021.

[2] A. Hammoudi, K. Moussaceb, C. Belebchouche, and F. Dahmoune, "Comparison of artificial neural network (ANN) and response surface methodology (RSM) prediction in compressive strength of recycled concrete aggregates," *Construction and Building Materials*, vol. 209, pp. 425–436, 2019.

[3] A. Poorarbabi, M. Ghasemi, M. Azhdary Moghaddam, and Moghaddam, "Concrete compressive strength prediction using non-destructive tests through response surface methodology," *Ain Shams Engineering Journal*, vol. 11, no. 4, pp. 939–949, 2020.

[4] S. M. A. Boukli Hacene, F. Ghomari, F. Schoefs, and A. Khelidj, "Probabilistic modelling of compressive strength of concrete using response surface methodology and neural networks," *Arabian Journal for Science and Engineering*, vol. 39, no. 6, pp. 4451–4460, 2014.

[5] A. Poorarbabi, M. Ghasemi, and M. Azhdary Moghaddam, "Concrete compressive strength prediction using neural networks based on non-destructive tests and a self-calibrated response surface methodology," *Journal of Nondestructive Evaluation*, vol. 39, pp. 78–10, 2020.

[6] A. A. Busari, W. K. Kupolati, J. M. Ndambuki et al., "Response surface analysis of the corrosion effect of metakaolin in reinforced concrete," *Silicon*, vol. 13, no. 7, pp. 2053–2061, 2020.

[7] G. K. Febin, A. Abhirami, A. K. Vineetha et al., "Strength and durability properties of quarry dust powder incorporated concrete blocks," *Construction and Building Materials*, vol. 228, Article ID 116793, 9 pages, 2019.

[8] M. S. Islam and S. Ju Ahmed, "Influence of jute fiber on concrete properties," *Construction and Building Materials*, vol. 189, pp. 768–776, 2018.

[9] C. K. Kankam, B. K. Meisuh, G. Sossou, and T. K. Buabin, "Stress-strain characteristics of concrete containing quarry rock dust as partial replacement of sand," *Case Studies in Construction Materials*, vol. 7, pp. 66–72, 2017.

[10] J. Sridhar, R. Gobinath, and M. S. Kirgiz, "Comparative study for efficacy of chemically treated jute fiber and bamboo fiber on the properties of reinforced concrete beams," *Journal of Natural Fibers*, vol. 19, no. 15, pp. 12224–12234, 2022.

[11] J. Dhanapal and S. Jeyaprakash, "Mechanical properties of mixed steel fiber reinforced concrete with the combination of micro and macro steel fibers," *Structural Concrete*, vol. 21, no. 1, pp. 458–467, 2019.

[12] J. Sridhar and D. Vivek, "Influence of non-biodegradable wastes on mechanical properties of concrete – a Neural Network approach," *IOP Conference Series: Materials Science and Engineering*, vol. 1025, Article ID 012007, 9 pages, 2021.

[13] K. S. Prasath, T. Tamilselvan, and R. Manobala, "Experimental investigation on mechanical and durability properties of concrete incorporated with quarry dust," *International Research Journal of Engineering and Technology*, vol. 6, no. 1, pp. 1610–1614, 2019.

[14] S. Tiwari, A. K. Sahu, and R. P. Pathak, "Mechanical properties and durability study of jute fiber reinforced concrete," *IOP Conference Series: Materials Science and Engineering*, vol. 961, Article ID 012009, 14 pages, 2020.

[15] M. Monsalve, O. Higuera, P. Estrada, M. Orozco, and C. Pedraza, "Production of structural type mortars reinforced with coconut fibre (coconuts nuciferas)," *Contemporary Engineering Sciences*, vol. 11, no. 85, pp. 4211–4218, 2018.

[16] T. Zhang, Y. Yin, Y. Gong, and L. Wang, "Mechanical properties of jute fibre-reinforced high-strength concrete," *Structural Concrete*, vol. 12, pp. 1–10, 2019.

[17] A. Conforti, R. Zerbino, and G. A. Plizzari, "Influence of steel, glass and polymer fibers on the cracking behavior of reinforced concrete beams under flexure," *Structural Concrete*, vol. 9, pp. 1–11, 2018.

[18] F. Ortiz-Navas, J. Navarro-Gregori, G. E. Leiva-Herdocia, P. Serna, and E. Cuenca, "An experimental study on the shear behaviour of reinforced concrete beams with macro synthetic fibres," *Construction and Building Materials*, vol. 169, pp. 888–899, 2018.

[19] T. Jirawattanasomkul, T. Ueda, S. Likitlersuang et al., "Effect of natural fibre reinforced polymers on confined compressive strength of concrete," *Construction and Building Materials*, vol. 223, pp. 156–164, 2019.

[20] F. K. Ksal, F. Altun, I. . Yig, and Y. Sahin, "Combined effect of silica fume and steel fiber on the mechanical properties of high strength concretes," *Construction and Building Materials*, vol. 22, pp. 1874–1880, 2018.

[21] P. K. Pasnur and S. B. Shetye, "Effect of blend of silica fume and sisal fiber on performance of concrete," *Journal of Advances in Scholarly Researches and Allied Education*, vol. 15, pp. 641–647, 2018.

[22] J. Ahmad, M. M. Arbili, A. Majdi, F. Althoey, A. Farouk Deifalla, and C. Rahmawati, "Performance of concrete reinforced with jute fibers (natural fibers): a review," *Journal of Engineered Fibers and Fabrics*, vol. 17, Article ID 155892502211218, 17 pages, 2022.

[23] J. Ahmad, A. Majdi, A. Al-Fakih et al., "Mechanical and durability performance of coconut fiber reinforced concrete: a state-of-the-art review," *Materials*, vol. 15, no. 10, pp. 3601–3624, 2022.

[24] M. Aziminezhad, M. Mahdikhani, and M. M. Memarpour, "RSM-based modeling and optimization of self-consolidating mortar to predict acceptable ranges of rheological properties," *Construction and Building Materials*, vol. 189, pp. 1200–1213, 2018.

[25] T. Awolusi, O. Oke, O. Akinkurolere, and A. O. Sojobi, "Application of response surface methodology: predicting and optimizing the properties of concrete containing steel fibre extracted from waste tires with limestone powder asFiller," *Case Studies in Construction Materials*, vol. 10, Article ID e00212, 2019.

[26] M. Esfahanian, M. Nikzad, G. Najafpour, and A. Ghoreyshi, "Modeling and optimization of ethanol fermentation using Saccharomyces cerevisiae: response surface methodology and artificial neural network," *Chemical Industry and Chemical Engineering Quarterly*, vol. 19, no. 2, pp. 241–252, 2013.

[27] S. J. S. Chelladurai, R. Arthanari, A. N. Thangaraj, and H. Sekar, "Dry sliding wear characterization of squeeze cast LM13/FeCu composite using response surface methodology," *China Foundry*, vol. 14, no. 6, pp. 525–533, 2017.

[28] C. Samson Jerold Samuel and A. Ramesh, "Investigation on microstructure and tensile behaviour of stir cast LM13 aluminium alloy reinforced with copper coated short steel fibres using response surface methodology," *Tran Indian Inst Met*, vol. 71, no. 9, pp. 2221–2230, 2018.

[29] Y. Moodi, S. R. Mousavi, A. Ghavidel, M. R. Sohrabi, and M. Rashki, "Using response surface methodology and providing a modified model using whale algorithm for estimating the compressive strength of columns confined with FRP sheets," *Construction and Building Materials*, vol. 183, pp. 163–170, 2018.

[30] U. Alaneme George and M. Mbadike Elvis, "Modelling of the mechanical properties of concrete with cement ratio partially replaced by aluminium waste and sawdust ash using artificial neural network," *SN Applied Sciences*, vol. 1, no. 11, Article ID 1514, 2019.

[31] Bureau of Indian Standards, *IS12269- Ordinary Portland Cement 53 Grade-Specification*, Bureau of Indian Standards, Manak Bhawan Old Delhi, 2013.

[32] Bureau of Indian Standards, *IS10262– Concrete Mix Proportioning -Guidelines*, Bureau of Indian Standards, Manak Bhawan Old Delhi, 2019.

[33] B. Animesh and D. Biswajit Saha, "Fabrication of PANI @Fe–Mn–Zr hybrid material and assessments in sono-assisted adsorption of methyl red dye: uptake performance and response surface," *Optimization*, vol. 99, no. 9, Article ID 100635, 2022.

[34] M. Adamu, M. L. Marouf, Y. E. Ibrahim, O. S. Ahmed, H. Alanazi, and A. L. Marouf, "Modeling and optimization of the mechanical properties of date fiber reinforced concrete containing silica fume using response surface methodology," *Case Studies in Construction Materials*, vol. 17, Article ID e01633, 22 pages, 2022.

[35] P. Das, S. Nisa, A. Debnath, and B. Saha, "Enhanced adsorptive removal of toxic anionic dye by novel magnetic polymeric nanocomposite: optimization of process parameters," *Journal of Dispersion Science and Technology*, vol. 43, no. 6, pp. 880–895, 2020.

[36] A. Deb, A. Debnath, and B. Saha, "Sono-assisted enhanced adsorption of eriochrome Black-T dye onto a novel polymeric nanocomposite: kinetic, isotherm, and response surface methodology optimization," *Journal of Dispersion Science and Technology*, vol. 42, no. 11, pp. 1579–1592, 2020.

[37] P. Das and A. Debnath, "Reactive orange 12 dye adsorption onto magnetically separable CaFe2O4 nanoparticles synthesized by simple chemical route: kinetic, isotherm and neural network modeling," *Water Practice and Technology*, vol. 16, no. 4, pp. 1141–1158, 2021.

[38] M. Bhowmik, A. Debnath, and B. Saha, "Fabrication of mixed phase CaFe2O4 and MnFe2O4 magnetic nanocomposite for enhanced and rapid adsorption of methyl orange dye: statistical modeling by neural network and response surface methodology," *Journal of Dispersion Science and Technology*, vol. 41, no. 13, pp. 1937–1948, 2019.

[39] M. Bhowmik, K. Deb, A. Debnath, and B. Saha, "Mixed phase Fe2O3/Mn3O4 magnetic nanocomposite for enhanced adsorption of methyl orange dye: neural network modeling and response surface methodology optimization," *Applied Organometallic Chemistry*, vol. 32, no. 3, 17 pages, Article ID e4186, 2017.

[40] M. Zakaria, M. Ahmed, M. M. Hoque, and S. Islam, "Scope of using jute fiber for the reinforcement of concrete material," *Textiles and Clothing Sustainability*, vol. 2, no. 1, p. 11, 2016.